

See discussions, stats, and author profiles for this publication at: <https://www.researchgate.net/publication/7828263>

ZnII–Salphen Complexes as Versatile Building Blocks for the Construction of Supramolecular Box Assemblies

ARTICLE *in* CHEMISTRY · AUGUST 2005

Impact Factor: 5.73 · DOI: 10.1002/chem.200500227 · Source: PubMed

CITATIONS

111

READS

31

6 AUTHORS, INCLUDING:



Mark Kuil

Cabot Corporation

25 PUBLICATIONS 911 CITATIONS

SEE PROFILE



Anthony L. Spek

Utrecht University

1,591 PUBLICATIONS 54,432 CITATIONS

SEE PROFILE



Joost N H Reek

University of Amsterdam

382 PUBLICATIONS 10,639 CITATIONS

SEE PROFILE

Zn^{II}–Salphen Complexes as Versatile Building Blocks for the Construction of Supramolecular Box Assemblies

Arjan W. Kleij,^[a] M. Kuil,^[a] Duncan M. Tooke,^[b] Martin Lutz,^[b] Anthony L. Spek,^[b] and Joost N. H. Reek^{*[a]}

Abstract: Zn^{II}–salphen complexes are readily accessible and interesting supramolecular building blocks with a large structural diversity. Higher-order supramolecular assemblies, such as molecular boxes based on a bis-Zn^{II}–salphen building block and various ditopic bipyridine ligands, have been constructed by means of supramolecular, coordinative Zn^{II}–N_{pyr} interactions. The use of bipyridine ligands of differing sizes enables the construction of structures with predefined box diameters. The features of the 2:2 box assemblies were investigated in detail by (variable temperature) NMR spectroscopy, UV-visi-

ble spectroscopy, NMR titrations, and X-ray crystallographic studies. The spectroscopic studies reveal a high association constant for the Zn^{II}–salphen–pyridyl motif, which lies in the range 10⁵–10⁶ M^{−1}. The strong interaction between the Zn^{II} center and pyridine donors was supported by PM3 calculations that showed a relatively high Lewis acid character of the metal center in the salphen complex. Titrations

curves monitored by UV-visible show a cooperative effect between the two bipyridine ligands upon complexation to the bis-Zn^{II} template, suggesting the formation of 2:2 complexes. The crystal structures of two supramolecular boxes have been determined. In both examples such a 2:2 assembly is present in the solid state, and the box size is different because they consist of different building blocks. Interestingly, the box assemblies line up in the solid state to form porous channels that are potentially useful in a number of applications.

Keywords: molecular boxes • porous materials • self-assembly • supramolecular chemistry • zinc

Introduction

Metalloporphyrin building blocks are widely used in supramolecular chemistry^[1] and are of special interest in the design of synthetic models for natural light-harvesting architectures.^[2] In the field of supramolecular chemistry, the pyridine–zinc(II)porphyrin interaction has been explored intensively and has been shown to be a valuable motif in the construction of discrete assemblies as well as oligomeric and

multiporphyrin arrays.^[3] Symmetrical, *meso*-phenyl-substituted porphyrin synthons are readily available; however, asymmetrically substituted porphyrins and chiral porphyrins are much less accessible and are generally only obtained in low quantities by means of tedious synthetic procedures. The development of novel molecular building blocks that address these issues would greatly stimulate the progress in this exciting research area.

Salen^[4] and salphen complexes have been studied extensively as homogeneous catalysts that exhibit great similarities with their porphyrin analogues.^[5] Much to our surprise, the pyridine–zinc(II)salphen interaction (salphen = *N,N'*-phenylenebis(salicylideneimine)) has not yet been explored in great detail as a binding motif, despite their great structural resemblance with porphyrins. The solid-state structure of a pyridyl–zinc(II)salen complex has been reported,^[6] and Hupp et al. proposed the use of axial ligation in rhenium-based box structures. However, owing to the limited solubility of these supramolecular structures, only fluorescence titrations have been performed.^[7a] In this contribution, we will demonstrate the synthetic accessibility of Zn^{II}–salphen complexes and we will show that these are indeed versatile

[a] Dr. A. W. Kleij, M. Kuil, Dr. J. N. H. Reek
Van't Hoff Institute for Molecular Sciences
University of Amsterdam
Nieuwe Achtergracht 166, 1018 WV, Amsterdam (The Netherlands)
Fax: (+31) 20-525-6422
E-mail: reek@science.uva.nl

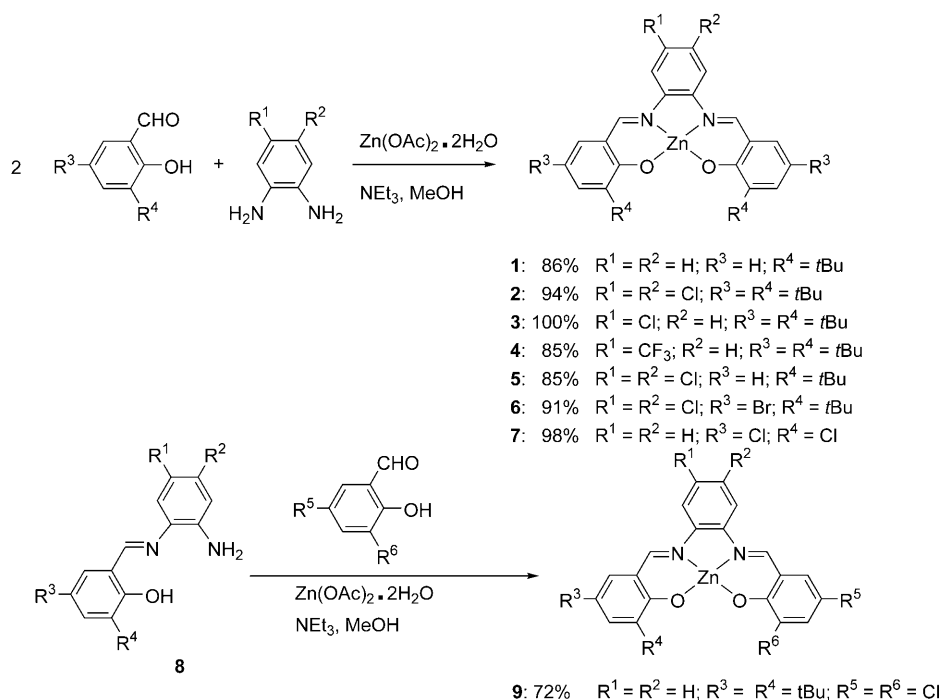
[b] Dr. D. M. Tooke, Dr. M. Lutz, Prof. Dr. A. L. Spek
Bijvoet Center for Biomolecular Research
Department of Crystal and Structural Chemistry
University of Utrecht
Padualaan 8, 3584 CH, Utrecht (The Netherlands)

Supporting information for this article is available on the WWW under <http://www.chemeurj.org/> or from the author.

building blocks in supramolecular chemistry, as is illustrated by the facile formation of open molecular box structures.^[7]

Results and Discussion

Synthesis of Zn^{II}-salphen building blocks: A zinc-mediated, one-pot, two-step procedure provides access to multigram quantities of a series of Zn^{II}-salphen complexes (**1–9**, Scheme 1) with variable steric and electronic properties.^[8]



Scheme 1. Synthesis of Zn^{II}-salphen building blocks **1–9**.

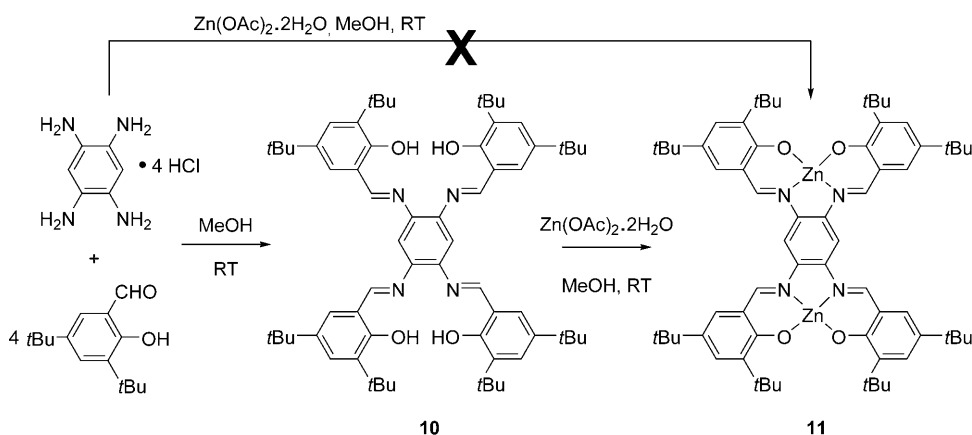
The products were all isolated as pure compounds by a simple filtration step, and were fully characterized by common spectroscopic techniques (see the Experimental Section). Nonsymmetrically substituted analogues were prepared by a two-step procedure after isolation of the previously described monoimine intermediate (Scheme 1).^[9] Under suitable reaction conditions, that is, in the presence of zinc(II) acetate and one equivalent of an aldehyde precursor, we did not observe any scrambling, and product **9** was also isolated simply by filtration.

Interestingly, mass spectro-metric studies of these Zn-salphen derivatives not only showed the peak corresponding

to the molecular weight of the compound, but also one belonging to the complex with axially ligated N-donor ligands, such as acetonitrile and pyridine, indicating a strong affinity in solution (for a typical example, see the Supporting Information). X-ray crystallographic^[10] measurements confirmed the identity of some of these complexes in which the nitrogen donor atoms are coordinated to the axial position of the zinc(II) atom.

Synthesis of bis-Zn^{II}-salphen complex **11:** The synthesis of bis-Zn^{II} complex **11** (Scheme 2) was first attempted following the one-pot, two-step approach with 3,5-di(*tert*-butyl)salicylaldehyde, 1,2,4,5-tetraaminobenzene tetrahydrochloride, and Zn(OAc)₂ in MeOH in analogy to **1–9**. This afforded a mixture of unidentified species, as indicated by NMR analysis. Therefore, the simple one-pot procedure seems to be limited to mono-Zn^{II}-salphen complexes. The synthesis of bimetallic **11** was eventually achieved via tetra-Schiff base precursor **10** (76% yield, Scheme 2),^[11] and subsequent introduction of the metal center by treatment with Zn(OAc)₂ in MeOH. However, extraction of the crude product followed by NMR analysis revealed the presence of a number of different species that were associated with oligomeric/polymeric structures. Apparently, under these conditions,

the formation of intermolecularly linked salphen segments is relatively more favorable than the intramolecular metalation process. The procedure was therefore carried out under



Scheme 2. Synthesis of bis-Zn^{II}-salphen complex **11**.

dilute conditions, and this furnished bis-Zn^{II} complex **11** (Scheme 2) as a red solid in 75 % yield after recrystallization from CH₃CN.

Binding, NMR, and modeling studies: UV-visible titration experiments in toluene revealed a very high binding constant for the assembly **2**·pyridine ($K_{\text{ass}} = 8.0 \times 10^5 \text{ M}^{-1}$),^[12] which is two orders of magnitude higher than that of the association of pyridine to Zn^{II}TPP ($6.1 \times 10^3 \text{ M}^{-1}$).^[13] Interestingly, an association constant of $1.2 \times 10^6 \text{ M}^{-1}$ was determined for **6**·pyridine; this illustrates that the stability of the complex can be fine-tuned by installing electron-withdrawing groups on the salphen structure. ¹H NMR titration experiments of **2** with pyridine in [D₆]acetone indicated a reasonable binding constant ($3.3 \times 10^3 \text{ M}^{-1}$) in a competing polar solvent.^[14] In contrast to the use of zinc(II)porphyrins, the formation of assemblies with zinc(II)salphen is not limited to apolar solvents! Whereas the complex-induced shifts can be spectacularly large for porphyrin-based assemblies owing to the large ring-current effects involved, in the Zn^{II}–salphen–pyridine complex, we found a typical shift of $\Delta\delta = 0.17 \text{ ppm}$ for the *ortho*-pyridyl proton. Similarly to the porphyrin assemblies, we found a rapid exchange of bound and free species on the NMR timescale, but the binding constant is much higher. Molecular modeling (PM3 calculations, Figure 1) qualitatively explains the difference between

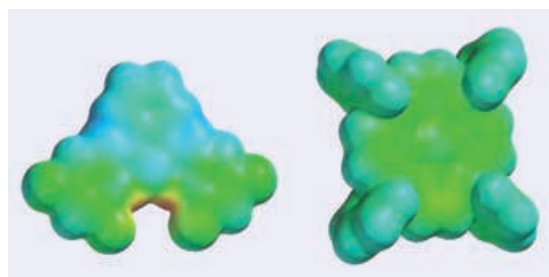
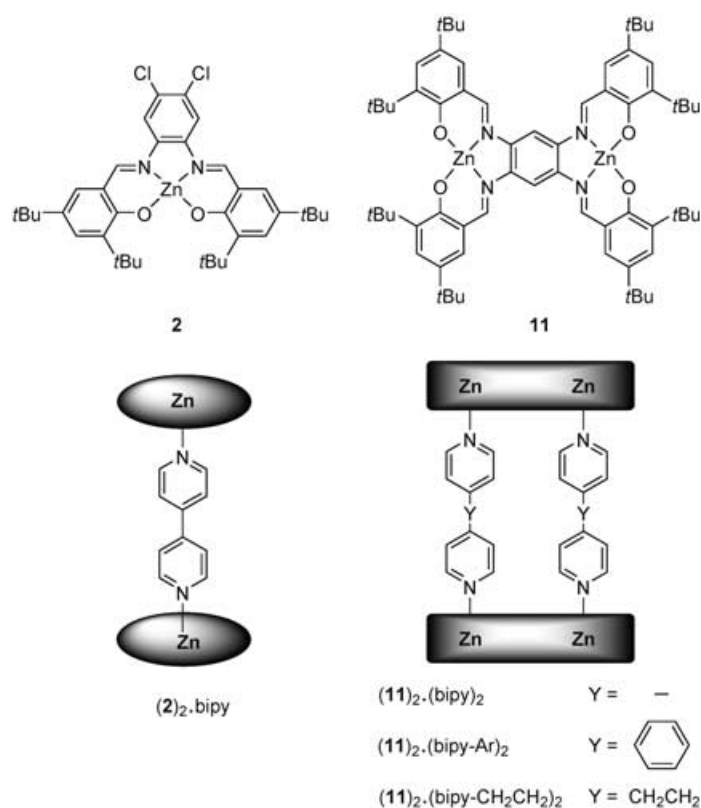


Figure 1. Potential energy surfaces calculated with PM3 showing the higher Lewis acidity (blue) of the Zn^{II} center in the salphen derivative **2** (left) compared to that in Zn^{II}TPP (green).

Zn^{II}TPP and the Zn^{II}–salphen complex: the zinc atom is far more positively charged in the Zn^{II}–salphen complex, and the potential energy surface shows a maximum at the zinc atom and aromatic ring, whereas it is much more delocalized on the Zn^{II}–porphyrin compound. As a result, the Zn^{II} center in the salphen complexes has a higher Lewis acid character, which results in stronger axial coordination. The calculated Mulliken charges of the zinc atom in the Zn^{II}–salphen complex and the Zn^{II}–porphyrin compound are 0.28 and –0.06, respectively.

The formation of larger assemblies was investigated with 4,4'-bipyridine as a ditopic ligand system (Scheme 3) by means of UV-visible titration experiments (toluene) and ¹H NMR spectroscopy (in [D₆]acetone!). The ¹H NMR spectrum of a mixture of **2** and 4,4'-bipyridine (2:1 stoichi-



Scheme 3. Schematic view of the higher-order supramolecular structures (**2**)₂·bipy and (**11**)₂·(bipy)₂, (**11**)₂·(bipy-Ar)₂, and (**11**)₂·(bipy-CH₂CH₂)₂.

ometry) pointed to the formation of a 2:1 assembly because the upfield shift of the Pyr-H_{ortho} ($\Delta\delta = 0.21 \text{ ppm}$) is similar to that observed for the assembly **2**·pyridine. The UV-visible titration curve for **2** and 4,4'-bipyridine showed an inflection point at a ratio of **2**/bipy=2, which also points to ditopic binding at 4,4'-bipyridine. As expected from two independent binding sites, a second inflection point at a ratio of **2**/bipy=1 was observed. The binding curve was fitted with a 2:1 model, showing virtually identical association constants for the first ($K_1 = 5.0 \times 10^5 \text{ M}^{-2}$) and second binding ($K_2 = 5.1 \times 10^5 \text{ M}^{-2}$) of **2** to the bipy ligand.^[12] The formation of a 2:1 assembly was unambiguously proven by X-ray crystallography (vide infra and Figure 2).^[15,16]

In order to arrive at more relevant supramolecular structures, we used bis-Zn^{II}–salphen **11** (Scheme 3), which, in combination with ditopic ligands, was anticipated to give neutral open-box assemblies. In contrast to **2**, the UV-visible titration curve of **11** and 4,4'-bipyridine showed only one inflection point at a ratio of **11**/bipy=1, suggesting that a single species is present with a very high overall binding constant. Although we were unable to fit the titration curve, we know that the overall association constant (for the (**11**)₂·(bipy)₂ complex) is at least 10^{20} M^{-3} because, at a concentration of $1.1 \times 10^{-5} \text{ M}$, more than 95 % is in the associated state. This is consistent with the cooperative binding of two bipy ligands in the 2:2 assembly, and is clearly sufficiently strong to suppress the formation of other assemblies (i.e., polymer-

ic structures). As for the $(\mathbf{2})_2\cdot\text{bipy}$ assembly, the ^1H NMR spectrum of the box in $[\text{D}_2]\text{dichloromethane}$ as well as in $[\text{D}_8]\text{toluene}$ displayed sharp peaks with the typical upfield shift for the 4,4'-bipyridine $\Delta\delta(\text{Pyr-H}_{ortho})=0.19$ ppm. Interestingly, in $[\text{D}_8]\text{toluene}$, the 4,4'-bipyridine *meta* proton was slightly broadened and the upfield shift was much larger compared to that observed in $[\text{D}_2]\text{dichloromethane}$ ($\Delta\delta\sim 0.4$ ppm in $[\text{D}_8]\text{toluene}$ compared to $\Delta\delta\sim 0.12$ ppm in $[\text{D}_2]\text{dichloromethane}$), probably as a result of the occupancy of the box by $[\text{D}_8]\text{toluene}$. At higher temperatures ($+60^\circ\text{C}$), the spectra did not change significantly and at temperatures lower than -20°C the bipy signals virtually disappeared owing to coalescence.^[17] ^1H NMR studies ($[\text{D}_8]\text{toluene}$) at different ratios of $\mathbf{11}$ and bipy ($\mathbf{11}/\text{bipy}=2, 1, \text{ and } 0.5$) showed that the box assembly is in fast exchange with the excess of free building block because sharp average resonances were observed in all cases. These fast-exchange features were generally observed for all pyridine-based assemblies in this work (vide supra). To demonstrate the versatility of the current approach to make box-type structures, we used two extended bipy ligands as ditopic components (i.e., 1,4-bis(4-pyridyl)benzene and 1,2-bis(4-pyridyl)ethane) thereby forming box structures with a larger diameter ($(\mathbf{11})_2\cdot(\text{bipy-Ar})_2$ and $(\mathbf{11})_2\cdot(\text{bipy-CH}_2\text{CH}_2)_2$). The NMR behavior of these structures was similar to that of $(\mathbf{11})_2\cdot(\text{bipy})_2$, that is, sharp resonances and similar shifts upon complex formation. The UV-visible titration results (Supporting Information) indicated the formation of an assembly with a high association constant and a 2:2 ratio of the components ($>10^{20}\text{ M}^{-3}$). Conclusive evidence of the proposed box structure for assemblies $(\mathbf{11})_2\cdot(\text{bipy})_2$ and $(\mathbf{11})_2\cdot(\text{bipy-CH}_2\text{CH}_2)_2$ was provided by X-ray crystallography (Figures 3, 4, and 5), which will be described below.^[15,16]

X-ray crystallography: In agreement with the 1:2 stoichiometry of the $(\mathbf{2})_2\cdot\text{bipy}$ complex formed in solution, the solid-state structure clearly showed the formation of the expected complex with the two zinc(II)salphen building blocks at either end of the bipy ligand (Figure 2). The Zn–Zn distance between the two Zn^{II} –salphen units is 11.25 \AA . The structure is slightly tilted in the solid state with a dihedral angle of $20.40(6)^\circ$ between the N_2O_2 base planes of Zn1 and Zn2, respectively. This is ascribed to crystal packing effects; the salphen units intercalate causing steric interactions that are responsible for the bent structure. In the solid-state structure of $(\mathbf{2})_2\cdot\text{bipy}$, the Zn– N_{pyr} bond lengths (2.12 \AA) are significantly shorter than the Zn^{II}– N_{pyr} bond

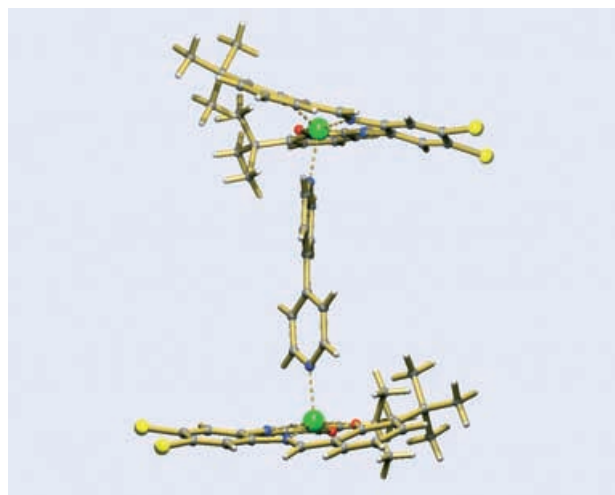


Figure 2. Molecular structure of the 2:1 assembly $(\mathbf{2})_2\cdot\text{bipy}$ in the solid state. Co-crystallized solvent molecules have been omitted for clarity (green = Zn, blue = N, yellow = Cl, red = oxygen, white = H, and gold = C).

length in the oligomeric, monopyridyl-substituted Zn^{II} TPP structure^[18] ($\text{Zn-N}=2.23\text{ \AA}$). This is in agreement with the higher association constant of pyridine to the more Lewis acidic Zn^{II} –salphen. The Zn^{II}– N_{pyr} bond lengths are similarly short in the other assemblies presented in this paper (for $(\mathbf{11})_2\cdot(\text{bipy})_2$: 2.14 and 2.11 \AA ; for $(\mathbf{11})_2\cdot(\text{bipy-CH}_2\text{CH}_2)_2$: 2.13 and 2.10 \AA).

The open-box structure proposed for assembly $(\mathbf{11})_2\cdot(\text{bipy})_2$ is clearly confirmed by the solid-state structure (Figure 3 left). The size of the molecular box is determined by the Zn–Zn distance within building block $\mathbf{11}$ on one hand (8.07 \AA) and on the other by the distance between the nitrogen donors of the ditopic ligand, which controls the distance between the two Zn^{II} –salphen units (11.33 \AA). This results

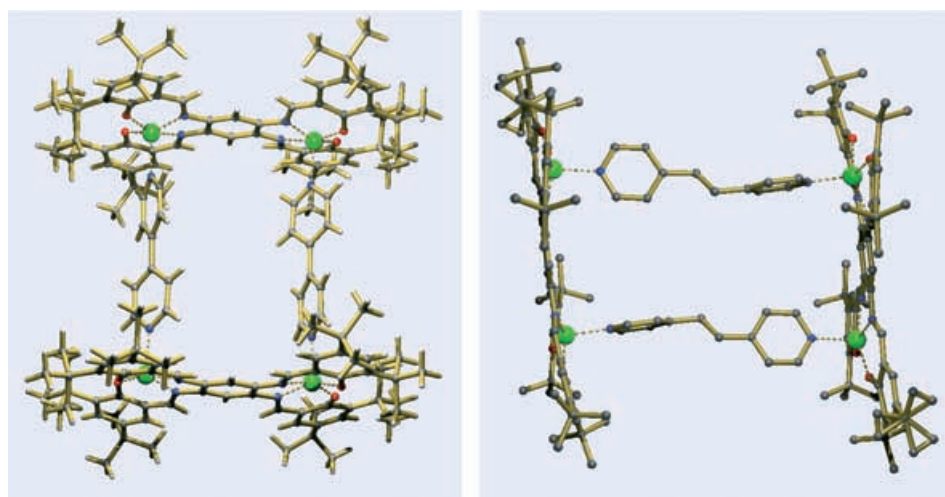


Figure 3. Molecular structures of assemblies of $(\mathbf{11})_2\cdot(\text{bipy})_2$ (left) and $(\mathbf{11})_2\cdot(\text{bipy-CH}_2\text{CH}_2)_2$ (right) in the solid state. Co-crystallized solvent molecules have been omitted for clarity (green = Zn, blue = N, yellow = Cl, red = oxygen, white = H, and gold = C).

in a box diameter of ~ 13.9 Å. Interestingly, the packing of the molecular boxes leads to a porous material with channels in one direction along the crystallographic *b* axis (Figure 4 top, for the porous structure of $(\mathbf{11})_2 \cdot (\text{bipy})_2$). It is

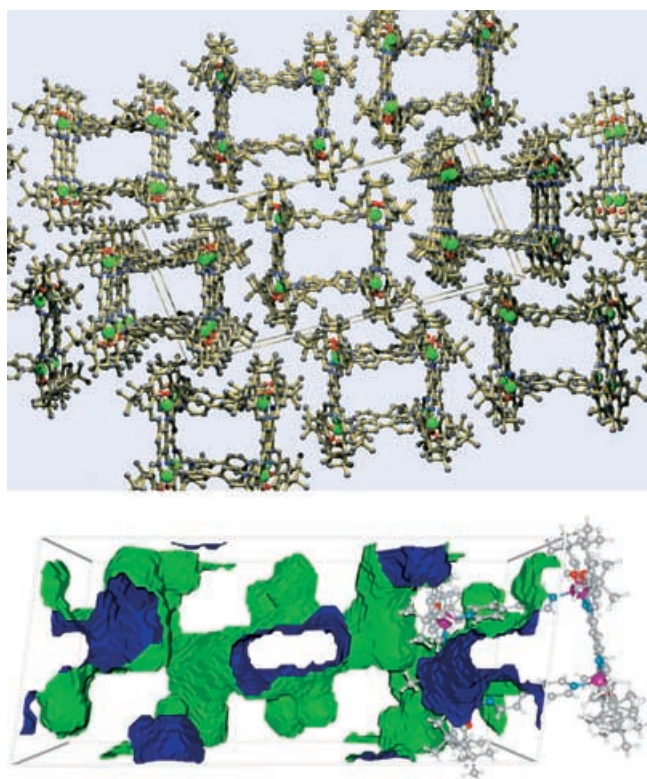


Figure 4. Top: Packing of $(\mathbf{11})_2 \cdot (\text{bipy})_2$ in the solid state, clearly showing the open channel structure (green = Zn, blue = N, red = oxygen, white = H, and gold = C; disordered solvent molecules occupying the channels have been omitted). Bottom: Solvent-accessible void in the unit cell of $(\mathbf{11})_2 \cdot (\text{bipy})_2$. The green and blue surfaces are the outsides and insides of the voids, respectively. The open-channel structure is clearly visible.^[28]

important to note that the box structures are formed by neutral building blocks and that the channels are not blocked by counterions but contain disordered solvent molecules (Figure 4 bottom). These materials are of great interest owing to their potential applications in molecular separation, heterogeneous catalysis, and storage.

In order to demonstrate the versatility of the molecular box approach, we also prepared crystals of assembly $(\mathbf{11})_2 \cdot (\text{bipy-CH}_2\text{CH}_2)_2$ that were suitable for X-ray diffraction experiments. These experiments again confirmed the open-box structure (Figure 3 right). Because only one of the components was larger, the box size was extended in one direction only, providing a molecular box size of 13.5×8.1 Å with a diameter of 15.7 Å. Because the ditopic ligand contains a flexible spacer, it adopts two slightly different conformations between the Zn^{II} -salphen units (only one is shown). Interestingly, the box structures again lined up in one dimension leading to the formation of porous solid materials; however, they now had different cavity dimensions

(Figure 5). The packing of this material seems slightly better since there is no solvent between the box arrays, in contrast to $(\mathbf{11})_2 \cdot (\text{bipy})_2$. The use of other ditopic ligands and bis- Zn^{II} -salphen building blocks should lead to porous materials with different controllable channel sizes. For example, molecular modeling predicts channel dimensions for $(\mathbf{11})_2 \cdot (\text{bipy-Ar})_2$ of 15.5×8 Å (diameter 17.4 Å).

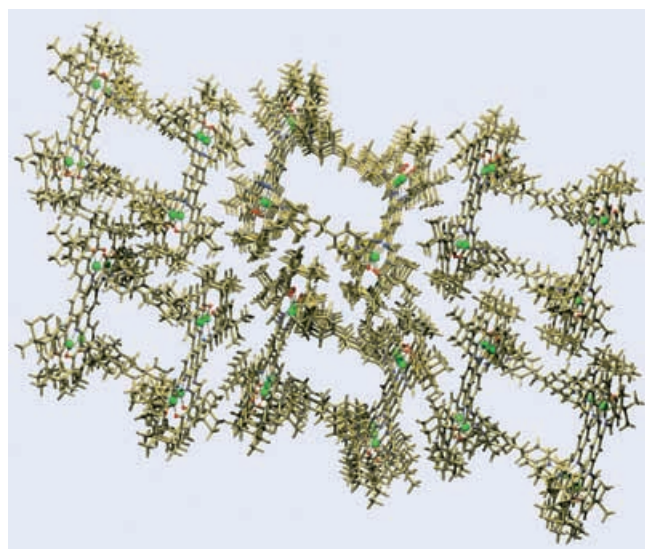


Figure 5. Packing of $(\mathbf{11})_2 \cdot (\text{bipy-CH}_2\text{CH}_2)_2$ in the solid state, the open-channel structure is formed by proper alignment of the supramolecular boxes (disordered solvent molecules occupying the channels have been omitted; green = Zn, blue = N, red = oxygen, white = H, and gold = C).

Conclusion

In summary, we have demonstrated that Zn^{II} -salphen complexes are excellent building blocks for the formation of supramolecular assemblies that utilize “pyridine–Zn” coordination motifs. Compared to the Zn^{II} TPP analogue, the binding constant between pyridine and Zn^{II} -salphens **2** and **6** is very high, even in competitive polar solvents such as acetone. Together with the facile access to a large variety of complexes, these Zn^{II} -salphen complexes provide highly interesting supramolecular building blocks for the construction of functional assemblies. Another striking feature is that the supramolecular complexes based on these building blocks readily crystallize, which facilitates structural analysis and enables the preparation of functional solid materials. As a first example of such an approach, we have prepared a small series of supramolecular boxes based on bis-salphen complex **11** that form porous materials in the solid state. It is worth noting that the bipy ligand, 1,2-bis(4-pyridyl)ethane, is relatively flexible and that the assembly is thus not limited to rigid building blocks. This thus enables access to peptide-based molecular boxes. We are currently exploring the use of these Zn^{II} -salphen complexes in functional porous materials^[19] and in the construction of supramolecular transition-metal catalyst assemblies based on Zn^{II} -salphen complexes

as noncatalytic building blocks through coordinative Zn^{II} - N_{pyr} interactions.^[20]

Experimental Section

Crystal structure determinations: X-ray intensities were collected on a Nonius KappaCCD diffractometer with rotating anode and $\text{MoK}\alpha$ radiation (graphite monochromator, $\lambda = 0.71073 \text{ \AA}$) at a temperature of 150(2) K. The data were corrected for absorption by SortAV^[21] ((**2**)₂-bipy and (**11**)₂-(bipy)₂) and SADABS^[22] ((**11**)₂-(bipy-CH₂CH₂)₂). The structures were solved by direct methods (SHELXS-97^[23] for (**2**)₂-bipy, SIR-97^[24] for (**11**)₂-(bipy)₂ and SHELXS-86 for (**11**)₂-(bipy-CH₂CH₂)₂) and refined with SHELXL-97^[24] against F^2 for all reflections. The drawings, structure calculations, and checking for higher symmetry were performed with the program PLATON.^[25] Disordered solvent molecules were taken into account by back-Fourier transformation with PLATON-SQUEEZE.^[26]

All standard reagents and solvents were commercially purchased and used as received. The reagent 5-bromo-3-*tert*-butylsalicylaldehyde^[27] was prepared according to a literature procedure. All NMR spectroscopic measurements were performed on a Mercury 300 MHz spectrometer at 25 °C with TMS as an external standard. Elemental analyses were carried out by Mikroanalytisch Laboratorium Dornis und Kolbe, Mülheim an der Ruhr (Germany). MS measurements were carried out in CH₃CN with a Shimadzu LCMS2010A spectrometer with atmospheric pressure chemical ionization.

Zn^{II}-salphen complex (1): A solution of *o*-phenylenediamine (0.57 g, 5.27 mmol), 3-*tert*-butylsalicylaldehyde (2.00 g, 11.2 mmol), Zn(OAc)₂·2H₂O (1.23 g, 5.60 mmol), and neat NEt₃ (2.0 mL) in MeOH (40 mL) was stirred for 18 h at room temperature. The desired compound was isolated by filtration and dried in vacuo to yield an orange solid (2.23 g, 86 %). ¹H NMR (300 MHz, [D₆]acetone): $\delta = 9.05$ (s, 2H; imine-H), 7.92–7.86 (m, 2H; Ar-H), 7.39–7.33 (m, 2H; Ar-H), 7.27 (dt, ⁴*J*(H,H) = 1.8, ³*J*(H,H) = 7.5 Hz, 4H; Ar-H), 6.48 (t, ³*J*(H,H) = 7.5 Hz, 2H; Ar-H), 1.52 ppm (s, 18H; C(CH₃)₃); ¹³C{¹H} NMR (75 MHz, [D₂]dichloromethane/[D₅]pyridine 95:5): $\delta = 173.44$, 162.96, 143.21, 140.58, 134.69, 131.48, 127.42, 119.95, 116.10, 113.19 (10 × Ar-C and imine-C), 35.87 (C(CH₃)₃), 29.85 ppm (C(CH₃)₃); UV/Vis ($c = 1.039 \text{ mg in 50 mL toluene}$): λ_{max} (ϵ) = 420 nm (17400 mol⁻¹ m³ cm⁻¹); MS (LC–MS, direct inlet, CH₃CN, APCI): m/z : 637 [$M+H$]⁺, 678 [$M+H+CH_3CN$]⁺; elemental analysis calcd (%) for C₂₉H₃₂N₂O₂Zn: C 68.84, H 6.37, N 5.54; found: C 68.35, H 6.26, N 5.64.

Zn^{II}-salphen complex (2): This compound was prepared as for **1** from 4,5-dichloro-*o*-phenylenediamine (0.59 g, 3.33 mmol), 3,5-di(*tert*-butyl)salicylaldehyde (1.81 g, 7.72 mmol), Zn(OAc)₂·2H₂O (0.83 g, 3.78 mmol), and neat NEt₃ (2 mL) in MeOH (50 mL) to give an orange solid (2.11 g, 94 %). Crystals suitable for X-ray diffraction were obtained from CH₂Cl₂/MeOH. ¹H NMR (300 MHz, [D₆]acetone): $\delta = 9.15$ (s, 2H; imine-H), 8.13 (s, 2H; Ar-H), 7.46 (d, ⁴*J*(H,H) = 2.7 Hz, 2H; Ar-H), 7.28 (d, ⁴*J*(H,H) = 3.0 Hz, 2H; Ar-H), 1.53 (s, 18H; C(CH₃)₃), 1.31 ppm (s, 18H; C(CH₃)₃); ¹³C{¹H} NMR (75 MHz, [D₆]acetone): $\delta = 172.75$, 164.68, 142.65, 140.77, 135.34, 130.97, 130.73, 130.45, 130.13, 119.32, 118.61 (11 × ArC and imine-C), 36.34, 34.53 (2 × C(CH₃)₃), 31.78 ppm (C(CH₃)₃, other signal probably overlapping with residual solvent signal); UV/Vis ($c = 0.880 \text{ mg in 50 mL in toluene}$): λ_{max} (ϵ) = 439 nm (18500 mol⁻¹ m³ cm⁻¹); MS (LC–MS, direct inlet, CH₃CN, APCI): m/z : 673 [$M+H$]⁺, 714 [$M+H+CH_3CN$]⁺, 755 [$M+H+2CH_3CN$]⁺; elemental analysis calcd (%) for C₃₆H₄₄Cl₂N₂O₂Zn: C 64.24, H 6.59, N 4.16; found: C 64.35, H 6.49, N 4.21.

Zn^{II}-salphen complex (3): This compound was prepared analogously to **1** from 4-chloro-*o*-phenylenediamine (192.1 mg, 1.35 mmol), 3,5-di(*tert*-butyl)salicylaldehyde (629.2 mg, 2.68 mmol), Zn(OAc)₂·2H₂O (418.3 mg, 1.91 mmol), and neat NEt₃ (1.5 mL) in MeOH (40 mL). The isolation of **3** was accomplished by addition of two volumes of H₂O to the crude reaction mixture and isolation of the orange precipitate by filtration (quantitative yield). Analytically pure **3** was obtained by crystallization from Et₂O/pentane at –20 °C. ¹H NMR (300 MHz, [D₆]acetone): $\delta = 9.13$ (s,

1H; imine-H), 9.09 (s, 1H; imine-H), 7.96 (d, ⁴*J*(H,H) = 1.8 Hz, 1H; Ar-H), 7.92 (d, ³*J*(H,H) = 8.7 Hz, 1H; Ar-H), 7.45 (t, ⁴*J*(H,H) = 2.7 Hz, 1H; Ar-H), 7.32 (d, ⁴*J*(H,H) = 2.4, ³*J*(H,H) = 9.0 Hz, 1H; Ar-H), 7.30 (d, ⁴*J*(H,H) = 2.7 Hz, 1H; Ar-H), 7.24 (d, ⁴*J*(H,H) = 2.7 Hz, 1H; Ar-H), 1.53 (s, 18H; C(CH₃)₃), 1.32 ppm (s, 18H; C(CH₃)₃); ¹³C{¹H} NMR (75 MHz, [D₆]acetone): $\delta = 172.53$, 172.24, 164.44, 163.84, 142.54, 142.02, 139.66, 135.11, 135.05, 132.54, 130.63, 130.44, 130.19, 126.96, 119.32, 118.13, 116.83 (17 × ArC and imine-C, some signals overlapping), 36.33, 34.50 (2 × C(CH₃)₃), 31.83, 30.28 ppm (2 × C(CH₃)₃); UV/Vis ($c = 1.222 \text{ mg in 50 mL in toluene}$): λ_{max} (ϵ) = 433 nm (21500 mol⁻¹ m³ cm⁻¹); MS (LC–MS, direct inlet, CH₃CN, APCI): m/z : 637 [$M+H$]⁺, 678 [$M+H+CH_3CN$]⁺, 719 [$M+H+2CH_3CN$]⁺; elemental analysis calcd (%) for C₃₆H₄₅ClN₂O₂Zn: C 67.71, H 7.10, N 4.39; found: C 67.55, H 6.93, N 4.25.

Zn^{II}-salphen complex (4): This compound was prepared analogously to **1** from 4-trifluoromethyl-*o*-phenylenediamine (310.1 mg, 1.76 mmol), 3,5-di(*tert*-butyl)salicylaldehyde (832.2 mg, 3.55 mmol), Zn(OAc)₂·2H₂O (431.1 mg, 1.96 mmol), and neat NEt₃ (2 mL) in MeOH (50 mL). The isolation of **4** was accomplished as reported for **3** to furnish an orange solid (1.00 g, 85 %). Analytically pure **4** was obtained by crystallization from Et₂O/pentane at –20 °C. ¹H NMR (300 MHz, [D₆]acetone): $\delta = 9.27$ (s, 1H; imine-H), 9.19 (s, 1H; imine-H), 8.26 (s, 1H; Ar-H), 8.11 (d, ³*J*(H,H) = 8.7 Hz, 1H; Ar-H), 7.64 (d, ³*J*(H,H) = 8.7 Hz, 1H; Ar-H), 7.47 (t, ⁴*J*(H,H) = 2.7 Hz, 1H; Ar-H), 7.30 (d, ⁴*J*(H,H) = 2.7 Hz, 1H; Ar-H), 7.27 (d, ⁴*J*(H,H) = 2.4 Hz, 1H; Ar-H), 1.54 (s, 18H; C(CH₃)₃), 1.32 ppm (s, 18H; C(CH₃)₃); ¹³C{¹H} NMR (75 MHz, [D₆]acetone): $\delta = 172.90$, 172.54, 165.11, 164.80, 143.83, 142.67, 142.51, 141.13, 135.23, 135.15, 130.73, 130.62, 128.32, 127.90, 127.22, 123.50, 119.26, 117.34, 113.87 (19 (2 × ArC and imine-C, one signal probably overlapping), 36.26, 34.43 (2 × C(CH₃)₃), 31.72 ppm (C(CH₃)₃, other signal probably overlapping with residual solvent signal). CF₃-carbon not observed; ¹⁹F{¹H} NMR (282 MHz, [D₆]acetone): $\delta = -59.77$ ppm (CF₃); UV/Vis ($c = 1.208 \text{ mg in 50 mL toluene}$): λ_{max} (ϵ) = 438 nm (19400 mol⁻¹ m³ cm⁻¹); MS (LC–MS, direct inlet, CH₃CN, APCI): m/z : 671 [$M+H$]⁺, 712 [$M+H+CH_3CN$]⁺, 751 [$M+H+2CH_3CN$]⁺; elemental analysis calcd (%) for C₃₇H₄₅F₃N₂O₂Zn: C 66.12, H 6.75, N 4.17; found: C 65.78, H 6.70, N 4.02.

Zn^{II}-salphen complex (5): This compound was prepared analogously to **1** from 4,5-dichloro-*o*-phenylenediamine (0.51 g, 2.88 mmol), 3-*tert*-butylsalicylaldehyde (1.14 g, 6.40 mmol), Zn(OAc)₂·2H₂O (0.67 g, 3.05 mmol), and neat NEt₃ (1.5 mL) in MeOH (30 mL). Isolation of the product furnished an orange solid (1.38 g, 85 %). Crystals suitable for X-ray diffraction were obtained from CH₃CN. ¹H NMR (300 MHz, [D₃]acetonitrile): $\delta = 8.83$ (s, 2H; imine-H), 7.92 (s, 2H; Ar-H), 7.31 (d, ³*J*(H,H) = 7.2 Hz, 2H; Ar-H), 7.20 (d, ³*J*(H,H) = 6.3 Hz, 2H; Ar-H), 6.50 (t, ³*J*(H,H) = 7.8 Hz, 2H; Ar-H), 1.47 ppm (s, 18H; C(CH₃)₃); ¹³C{¹H} NMR (75 MHz, [D₆]acetone): $\delta = 174.57$, 165.00, 143.52, 140.89, 135.96, 132.55, 130.72, 120.74, 119.02, 114.32 (10 × ArC and imine-C), 36.34 ppm (C(CH₃)₃). The other *t*Bu-carbon signal is probably overlapping with residual solvent signal; UV/Vis ($c = 1.762 \text{ mg in 50 mL toluene}$): λ_{max} (ϵ) = 431 nm (18900 mol⁻¹ m³ cm⁻¹); MS (LC–MS, direct inlet, CH₃CN, APCI): m/z : 561 [$M+H$]⁺, 602 [$M+H+CH_3CN$]⁺, 643 [$M+H+2CH_3CN$]⁺; elemental analysis calcd (%) for C₂₈H₂₈Cl₂N₂O₂Zn·2½ H₂O: C 55.51, H 5.49, N 4.62; found: C 55.85, H 5.53, N 4.43 %.

Zn^{II}-salphen complex (6): This compound was prepared analogously to **1** from 4,5-dichloro-*o*-phenylenediamine (185.2 mg, 1.05 mmol), 3-*tert*-butyl-5-bromosalicylaldehyde (543.3 mg, 2.11 mmol), Zn(OAc)₂·2H₂O (269.9 mg, 1.23 mmol), and neat NEt₃ (1.5 mL) in MeOH (40 mL). The product was obtained by precipitation from Et₂O/pentane to furnish a dark orange solid (0.69 g, 91 %). ¹H NMR (300 MHz, [D₆]acetone): $\delta = 9.12$ (s, 2H; imine-H), 8.17 (s, 2H; ArH), 7.49 (d, ⁴*J*(H,H) = 2.7 Hz, 2H; ArH), 7.32 (d, ⁴*J*(H,H) = 2.7 Hz, 2H; ArH), 1.49 ppm (s, 18H; C(CH₃)₃); ¹³C{¹H} NMR (75 MHz, [D₆]acetone): $\delta = 172.61$, 163.84, 146.08, 140.32, 136.55, 134.72, 131.04, 121.72, 118.97, 104.57 (10 × ArC), 36.27 (C(CH₃)₃), 29.52 ppm (C(CH₃)₃); UV/Vis ($c = 1.654 \text{ mg in 50 mL toluene}$): λ_{max} (ϵ) = 439 nm (25200 mol⁻¹ m³ cm⁻¹); MS (LC–MS, direct inlet, CH₃CN, APCI): m/z : 719 [$M+H$]⁺, 760 [$M+H+CH_3CN$]⁺; elemental analysis calcd (%) for C₂₈H₂₆Cl₂BrN₂O₂Zn·CH₃CN: C 48.12, H 4.04, N 5.43; found: C 48.30, H 4.28, N 5.63.

Zn^{II}-salphen complex (7): This compound was prepared analogously to **1** from *o*-phenylenediamine (0.52 g, 4.81 mmol), 3,5-dichlorosalicylaldehyde (1.85 g, 9.69 mmol), Zn(OAc)₂·2H₂O (1.13 g, 5.15 mmol), and neat NEt₃ (5 mL) in MeOH/CH₂Cl₂ (50/150 mL). After 45 min, the product was isolated by filtration (2.43 g, 97 %). Crystals suitable for X-ray diffraction were obtained from CH₃CN/pyridine (≈25:1). ¹H NMR (300 MHz, [D₅]pyridine): δ = 8.45 (brs, 2H; imine-H), 7.32 (br, 4H; Ar-H), 7.14 (brs, 2H; Ar-H, partly overlapping with solvent signal), 6.95 ppm (brs, 2H; Ar-H); ¹³C{¹H} NMR (75 MHz, [D₅]pyridine): δ = 166.72, 163.11, 140.95, 134.26, 129.24, 121.69, 118.06, 116.49 ppm (8×ArC, two signals coinciding with solvent signal(s)); UV/Vis (c = 1.001 mg in 50 mL DMF): λ_{max} (ε) = 410 nm (22000 mol⁻¹m³cm⁻¹); MS (LC-MS, direct inlet, CH₃CN as eluent with added pyridine as co-eluent, APCI): m/z: 557 [M+H+CH₃CN]⁺, 616 [M+H+pyridine+H₂O]⁺, 1035 [2M+H]⁺; elemental analysis calcd (%) for C₂₀H₁₀Cl₄N₂O₂Zn: C 46.42, H 1.95, N 5.41; found: C 46.34, H 2.08, N 5.36.

Zn^{II}-salphen complex (9): This compound was prepared analogously to **1** from monoimine phensal(*t*Bu)H₃ (**8**, 454.2 mg, 1.40 mmol), 3,5-di-chloro-salicylaldehyde (267.1 mg, 1.40 mmol), Zn(OAc)₂·2H₂O (308.2 mg, 1.40 mmol), and neat NEt₃ (0.5 mL) in MeOH (50 mL). After 15 min, the mixture was filtered, and the bright orange solid was dried in vacuo. A second fraction was obtained by concentration of the mother liquor to give the product (0.65 g, 83 %). Crystals suitable for X-ray crystallography were obtained from CH₃CN. ¹H NMR (300 MHz, [D₆]acetone): δ = 8.97 (s, 1H; imine-H), 8.94 (s, 1H; imine-H), 7.83 (d, ³J(H,H) = 8.1 Hz, 2H; Ar-H), 7.45–7.38 (m, 5H; Ar-H), 7.18 (d, ⁴J(H,H) = 2.7 Hz, 1H; Ar-H), 1.50 (s, 9H; C(CH₃)₃), 1.29 ppm (s, 9H; C(CH₃)₃); ¹³C{¹H} NMR (75 MHz, [D₆]dichloromethane/[D₅]pyridine 95:5): δ = 171.94, 165.89 (2×imine-C), 164.19, 161.57, 142.53, 141.48, 139.80, 135.19, 133.54, 132.99, 130.46, 129.70, 128.80, 127.21, 120.68, 118.59, 116.76, 116.68, 116.34 (17×Ar-C), 36.01, 34.28 (2×C(CH₃)₃), 31.65, 29.82 ppm (2×C(CH₃)₃); UV/Vis (c = 1.120 mg in 50 mL toluene): λ_{max} (ε) = 403 nm (12200 mol⁻¹m³cm⁻¹); MS (LC-MS, direct inlet, CH₃CN, APCI): m/z: 561 [M+H]⁺, 602 [M+H+CH₃CN]⁺, 1121 [2M+H]⁺; elemental analysis calcd (%) for C₂₀H₃₀Cl₂N₂O₂Zn·2H₂O: C 57.02, H 5.61, N 4.59; found: C 56.51, H 5.65, N 4.62.

Bis-salphen-(Zn^{II})₂ complex (11): To a suspension of **10** (257.1 mg, 0.256 mmol) in MeOH (250 mL), a solution of Zn(OAc)₂·2H₂O (112.5 mg, 0.513 mmol) in MeOH (5 mL) was slowly added. After 68 h, the mixture was concentrated and extracted with CH₂Cl₂ (100 mL). Concentration and recrystallization of the crude product from CH₃CN yielded a red solid (216 mg, 75 %). ¹H NMR (300 MHz, [D₆]acetone): δ = 9.23 (s, 4H; imine-rH), 8.49 (s, 2H; ArH_{core}), 7.46 (s, 4H; ArH), 7.19 (s, 4H; ArH), 1.55 (s, 36H; C(CH₃)₃), 1.33 ppm (s, 36H; C(CH₃)₃); ¹³C{¹H} NMR (75 MHz, [D₆]acetone): δ = 172.17, 163.19, 142.44, 139.72, 134.95, 130.16, 130.03, 119.57 (8×Ar-C and imine-C, one signal missing probably due to overlap), 36.33, 34.45 (2×C(CH₃)₃), 31.85, 30.28 ppm (2×C(CH₃)₃); UV/Vis (c = 0.821 mg in 50 mL toluene): λ_{max} (ε) = 508 nm (55000 mol⁻¹m³cm⁻¹); MS (LC-MS, direct inlet, CH₃CN, APCI): m/z: 1130 [M+H]⁺; elemental analysis calcd (%) for C₆₆H₈₆N₄O₄Zn₂: C 70.14, H 7.67, N 4.96; found: C 69.76, H 7.78, N 4.91.

Acknowledgements

This research was sponsored by The Netherlands Organization for Scientific Research and the University of Amsterdam (NWO-VICI). ALS, ML, and DMT thank the Council for the Chemical Sciences of the Netherlands Organization for Scientific Research (CW-NWO) for their support.

- [1] a) P. J. Stang, J. Fan, B. Olenyuk, *Chem. Commun.* **1997**, 1453–1454; b) C.-T. Chen, *Comprehensive Supramolecular Chemistry*, Vol. 5, Pergamon, Oxford, **1996**; c) J. L. Sessler, B. Wang, S. L. Springs, C. T. Brown, *Comprehensive Supramolecular Chemistry*, Vol. 4, Pergamon, Oxford, **1996**; d) H. Tamiaki, *Coord. Chem. Rev.* **1996**, 148,

- 183–197; e) C. M. Drain, J.-M. Lehn, *J. Chem. Soc. Chem. Commun.* **1994**, 2313–2314; f) L. Di Constanzo, S. Geremia, L. Randaccio, R. Purello, R. Lauceri, D. Sciotto, F. G. Gulino, *Angew. Chem.* **2001**, 113, 4375–4377; *Angew. Chem. Int. Ed.* **2001**, 40, 4245–4247; g) G. Moschetto, R. Lauceri, F. G. Gulino, D. Sciotto, R. Purello, *J. Am. Chem. Soc.* **2002**, 124, 14536–14537; h) L. G. Mackay, R. S. Wylie, J. K. Sanders, *J. Am. Chem. Soc.* **1994**, 116, 3141–3142; i) M. Nakasg, Z. Clyde-Watson, N. Feeder, J. E. Davies, S. J. Teat, J. K. Sanders, *J. Am. Chem. Soc.* **2000**, 122, 5286–5293; j) J. Fan, J. A. Whiteford, B. Olenyuk, M. D. Levin, P. J. Stang, E. B. Fleischer, *J. Am. Chem. Soc.* **1999**, 121, 2741–2752.
- [2] a) R. A. Haycock, A. Yartsev, U. Michelsen, V. Sundström, C. A. Hunter, *Angew. Chem.* **2000**, 112, 3762–3765; *Angew. Chem. Int. Ed.* **2000**, 39, 3616–3619; b) C. A. Hunter, M. N. Meah, J. K. M. Sanders, *J. Chem. Soc. Chem. Commun.* **1988**, 692–694; c) J. Li, A. Ambroise, S. I. Yang, J. R. Diers, J. Seth, C. R. Wack, D. F. Bocian, D. Holtz, J. S. Lindsey, *J. Am. Chem. Soc.* **1999**, 121, 8927–8940.
- [3] a) K. Funatsu, T. Imamura, A. Ichimura, Y. Sasaki, *Inorg. Chem.* **1998**, 37, 4986–4995; b) Y. Kobuke, H. Miyaji, *J. Am. Chem. Soc.* **1994**, 116, 4111–4112; c) R. T. Stibrany, J. Vasudevan, S. Knapp, J. A. Potenza, T. Emge, H. J. Schugar, *J. Am. Chem. Soc.* **1996**, 118, 3980–3981; d) A. Okumura, K. Funatsu, Y. Sasaki, T. Imamura, *Chem. Lett.* **1999**, 779–780; e) L. J. Twyman, A. S. H. King, *Chem. Commun.* **2002**, 910–911; f) G. S. Wilson, H. L. Anderson, *Chem. Commun.* **1999**, 1539–1540.
- [4] For some reviews, see: a) L. Canali, D. C. Sherrington, *Chem. Soc. Rev.* **1999**, 28, 85–93; b) E. N. Jacobsen, *Acc. Chem. Res.* **2000**, 33, 421–431; c) T. Katsuki, *Coord. Chem. Rev.* **1995**, 140, 189–214; d) D. A. Atwood, M. J. Harvey, *Chem. Rev.* **2001**, 101, 37–52.
- [5] For some examples, see: a) E. N. Jacobsen, W. Zhang, M. L. Güler, *J. Am. Chem. Soc.* **1991**, 113, 6703–6704; b) G. M. Sammis, E. N. Jacobsen, *J. Am. Chem. Soc.* **2003**, 125, 4442–4443; c) A. G. Dosseter, T. F. Jamison, E. N. Jacobsen, *Angew. Chem.* **1999**, 111, 2549–2552; *Angew. Chem. Int. Ed.* **1999**, 38, 2398–2400; d) Z.-B. Li, L. Pu, *Org. Lett.* **2004**, 6, 1065–1068; e) S. K. Edulji, S. T. Nguyen, *Organometallics* **2003**, 22, 3374–3381.
- [6] a) A. L. Singer, D. A. Atwood, *Inorg. Chim. Acta* **1998**, 277, 157–162; b) G. A. Morris, H. Zhou, C. L. Stern, S. T. Nguyen, *Inorg. Chem.* **2001**, 40, 3222–3227.
- [7] Salen ligands/complexes appended with pyridine groups at the 3 and 3' positions have been recently used to construct loop- and square-type assemblies. The major difference with respect to the current approach is that in these studies the metal center of the salphen unit was not used to induce assembly formation. See: a) K. E. Splan, A. M. Massari, G. A. Morris, S.-S. Sun, E. Reina, S. T. Nguyen, J. T. Hupp, *Eur. J. Inorg. Chem.* **2003**, 2348–2351; b) S.-S. Sun, C. Stern, S. T. Nguyen, J. T. Hupp, *J. Am. Chem. Soc.* **2004**, 126, 6314–6326. For a recent study on the use of salphen ligands in supramolecular coordination polymers, see: c) R. Kitauro, G. Onoyama, H. Sakamoto, R. Matsuda, S.-I. Noro, S. Kitagawa, *Angew. Chem.* **2004**, 116, 2738–2741; *Angew. Chem. Int. Ed.* **2004**, 43, 2684–2687.
- [8] Please note that the isolation of the precursor ligands is not necessary with this approach and that asymmetrically substituted salphen-Zn complexes can be readily accessed.
- [9] M.-A. Muñoz-Hernández, T. S. Keizer, S. Parkin, B. Patrick, D. A. Atwood, *Organometallics* **2000**, 19, 4416–4421.
- [10] For recent examples of Zn^{II}-salphens with axial ligation, see: a) A. L. Singer, D. A. Atwood, *Inorg. Chim. Acta* **1998**, 277, 157–162; b) G. A. Morris, H. Zhou, C. L. Stern, S. T. Nguyen, *Inorg. Chem.* **2001**, 40, 3222–3227.
- [11] K. Chichak, U. Jacquemard, N. R. Branda, *Eur. J. Inorg. Chem.* **2002**, 357–368.
- [12] We examined the binding curves in the present studies with software developed by Prof. C. A. Hunter (Sheffield University, UK). See also: A. P. Bisson, C. A. Hunter, J. C. Morales, K. Young, *Chem. Eur. J.* **1998**, 4, 845–851.
- [13] V. F. Slagt, P. J. C. Kamer, P. W. N. M. van Leeuwen, J. N. H. Reek, *J. Am. Chem. Soc.* **2004**, 126, 1526–1536.

- [14] Note that the Zn^{II} -salphen complexes in this work proved to be unstable in the presence of relatively acidic solvents such as [D]chloroform.
- [15] Data for $(\mathbf{2})_2\text{bipy}$: $\text{C}_{66}\text{H}_{64}\text{Cl}_4\text{N}_6\text{O}_4\text{Zn}_2$ + disordered solvent, $M_r = 1277.77$ [*], orange block, $0.42 \times 0.30 \times 0.20 \text{ mm}^3$; monoclinic, $C2/c$ (no. 15); $a = 49.2838(3)$, $b = 13.3123(1)$, $c = 19.9761(1) \text{ \AA}$, $\beta = 106.7889(2)^\circ$, $V = 12547.30(14) \text{ \AA}^3$, $Z = 8$, $\rho = 1.353 \text{ g cm}^{-3}$ [*], $\mu = 0.987 \text{ mm}^{-1}$ [*]; 95 859 reflections were measured up to a resolution of $(\sin \theta/\lambda)_{\text{max}} = 0.65 \text{ \AA}^{-1}$. An absorption correction based on multiple measured reflections was applied (correction range 0.75–0.82); 14 431 reflections were unique ($R_{\text{int}} = 0.0568$). The crystal structure contained large voids (815 \AA^3 per unit cell) filled with disordered solvent molecules, amounting to 282 electrons per unit cell. Their contribution to the structure factors was secured by back-Fourier transformation with the SQUEEZE procedure in the program PLATON. 751 Refined parameters, no restraints; $R(\text{obsd reflections})$: $R1 = 0.0357$, $wR2 = 0.0973$; R (all data): $R1 = 0.0495$, $wR2 = 0.1044$; $\text{GOF} = 1.089$. Residual electron density between -0.59 and 0.49 e \AA^{-3} . Data for $(\mathbf{11})_2\text{-(bipy)}_2$: $\text{C}_{152}\text{H}_{188}\text{N}_{12}\text{O}_8\text{Zn}_4 + 2 \text{ C}_2\text{H}_3\text{N}$ + disordered solvent, $M_r = 2654.73$ [*], dark red block, $0.30 \times 0.28 \times 0.21 \text{ mm}^3$; monoclinic, $P2_1/c$ (no. 14); $a = 17.5988(1)$, $b = 13.0760(1)$, $c = 40.2384(4) \text{ \AA}$, $\beta = 97.4302(5)^\circ$, $V = 9181.98(13) \text{ \AA}^3$, $Z = 2$, $\rho = 0.960 \text{ g cm}^{-3}$ [*], $\mu = 0.564 \text{ mm}^{-1}$ [*]; 70 761 reflections were measured up to a resolution of $(\sin \theta/\lambda)_{\text{max}} = 0.60 \text{ \AA}^{-1}$. An absorption correction based on multiple measured reflections was applied (correction range 0.66–0.89); 11 997 reflections were unique ($R_{\text{int}} = 0.0750$). One *t*Bu group was refined with a disorder model. In addition to the ordered acetonitrile molecules, the crystal structure contained large voids (2708 \AA^3 per unit cell) filled with disordered solvent molecules, amounting to 707 electrons per unit cell. Their contribution to the structure factors was secured by back-Fourier transformation with the SQUEEZE procedure in the program PLATON. 876 Refined parameters, 81 restraints; $R(\text{obsd reflections})$: $R1 = 0.0519$, $wR2 = 0.1415$; R (all data): $R1 = 0.0681$, $wR2 = 0.1495$; $\text{GOF} = 1.043$; residual electron density between -0.50 and 0.84 e \AA^{-3} . Data for $(\mathbf{11})_2\text{-(bipy-CH}_2\text{CH}_2)_2$: $\text{C}_{156}\text{H}_{196}\text{N}_{12}\text{O}_8\text{Zn}_4$ + disordered solvent, $M_r = 2628.73$ [*], dark red block, $0.10 \times 0.10 \times 0.60 \text{ mm}^3$; monoclinic, $P2_1/c$ (no. 14); $a = 17.7604(8)$, $b = 12.8246(5)$, $c = 41.889(2) \text{ \AA}$, $\beta = 101.184(4)^\circ$, $V = 9359.9(7) \text{ \AA}^3$, $Z = 2$, $\rho = 0.933 \text{ g cm}^{-3}$ [*], $\mu = 0.552 \text{ mm}^{-1}$ [*]; 135 702 reflections were measured up to a resolution of $(\sin \theta/\lambda)_{\text{max}} = 0.54 \text{ \AA}^{-1}$. An absorption correction based on multiple measured reflections was applied (correction range 0.70–0.95). 12 242 Reflections were unique ($R_{\text{int}} = 0.052$). One *t*Bu group and the linking group were refined with a disorder model, with occupancies of 51 % and 49 % in both cases. In addition to the ordered acetonitrile molecules, the crystal structure contained large voids (2859 \AA^3 per unit cell) filled with disordered solvent molecules, amounting to 499 electrons per unit cell. 1003 Refined parameters, 499 restraints; $R(\text{obsd reflections})$: $R1 = 0.0519$, $wR2 = 0.1267$; R (all data): $R1 = 0.0640$, $wR2 = 0.1330$; $\text{GOF} = 1.037$; residual electron density between -0.50 and 0.61 e \AA^{-3} . Note that the asterisk behind some of the numerical, crystallographic data denote the values without the contribution of the disordered solvent molecules.
- [16] CCDC-244766 (compound $(\mathbf{2})_2\text{bipy}$), CCDC-244767 (compound $(\mathbf{11})_2\text{-(bipy)}_2$) and CCDC-264904 (compound $(\mathbf{11})_2\text{-(bipy-CH}_2\text{CH}_2)_2$) contain the supplementary crystallographic data for this paper. These data can be obtained free of charge from the Cambridge Crystallographic Data Centre via www.ccdc.cam.ac.uk/data_request/cif.
- [17] The slow-exchange region was not reached and must be below -60°C .
- [18] E. B. Fleischer, A. M. Shachter, *Inorg. Chem.* **1991**, *30*, 3763–3769.
- [19] For interesting reviews, see: a) S. Kitagawa, R. Kitaura, S.-I. Noro, *Angew. Chem.* **2004**, *116*, 2388–2430; *Angew. Chem. Int. Ed.* **2004**, *43*, 2335–2375; b) S. A. Barnett, N. R. Champness, *Coord. Chem. Rev.* **2003**, *246*, 145–168.
- [20] For the use of such interactions in catalyst assemblies based on Zn^{II} -porphyrin building blocks, see: a) V. F. Slagt, J. N. H. Reek, P. J. C. Kamer, P. W. N. M. van Leeuwen, *Angew. Chem.* **2001**, *113*, 4401–4403; *Angew. Chem. Int. Ed.* **2001**, *40*, 4271–4273; b) V. F. Slagt, P. J. C. Kamer, P. W. N. M. van Leeuwen, J. N. H. Reek, *J. Am. Chem. Soc.* **2004**, *126*, 4056–4057; c) G. A. Morris, S. T. Nguyen, J. T. Hupp, *J. Mol. Catal. A* **2001**, *174*, 15–20.
- [21] R. H. Blessing, *Acta Crystallogr. Sect. A* **1995**, *51*, 33–38.
- [22] G. M. Sheldrick, Bruker AXS, Karlsruhe (Germany), **2004**.
- [23] G. M. Sheldrick, SHELXS-97; Universität Göttingen, Göttingen (Germany), **1997**.
- [24] A. Altomare, M. C. Burla, M. Camalli, G. L. Cascarano, C. Giacovazzo, A. Guagliardi, A. G. G. Moliterni, G. Polidori, R. Spagna, *J. Appl. Crystallogr.* **1999**, *32*, 115–119.
- [25] A. L. Spek, *J. Appl. Crystallogr.* **2003**, *36*, 7–13.
- [26] P. van der Sluis, A. L. Spek, *Acta Crystallogr. Sect. A* **1990**, *46*, 194–201.
- [27] J. F. Larrow, E. N. Jacobsen, Y. Gao, Y. Hong, X. Nie, C. M. Zepp, *J. Org. Chem.* **1994**, *59*, 1939–1942.
- [28] D. M. Tooke, A. L. Spek, *Fourier3D software program*, *J. Appl. Cryst.*, submitted.

Received: February 28, 2005
Published online: May 24, 2005